



UNIVERSITY OF LEEDS

This is a repository copy of *The impact of source distribution on scalar transport over forested hills*.

White Rose Research Online URL for this paper:
<http://eprints.whiterose.ac.uk/85116/>

Version: Accepted Version

Article:

Ross, AN and Harman, IN (2015) The impact of source distribution on scalar transport over forested hills. *Boundary-Layer Meteorology*, 156 (2). pp. 211-230. ISSN 0006-8314

<https://doi.org/10.1007/s10546-015-0029-5>

Reuse

Unless indicated otherwise, fulltext items are protected by copyright with all rights reserved. The copyright exception in section 29 of the Copyright, Designs and Patents Act 1988 allows the making of a single copy solely for the purpose of non-commercial research or private study within the limits of fair dealing. The publisher or other rights-holder may allow further reproduction and re-use of this version - refer to the White Rose Research Online record for this item. Where records identify the publisher as the copyright holder, users can verify any specific terms of use on the publisher's website.

Takedown

If you consider content in White Rose Research Online to be in breach of UK law, please notify us by emailing eprints@whiterose.ac.uk including the URL of the record and the reason for the withdrawal request.



eprints@whiterose.ac.uk
<https://eprints.whiterose.ac.uk/>

1 **The impact of source distribution on scalar transport**
2 **over forested hills**

3 **Andrew N. Ross, Ian N. Harman**

4

5 April 15, 2015

6 **Abstract** Numerical simulations of neutral flow over a two-dimensional, iso-
7 lated, forested ridge are conducted to study the effects of scalar source distri-
8 bution on scalar concentrations and fluxes over forested hills. Three different
9 constant-flux sources are considered that span a range of idealized but ecolog-
10 ically important source distributions - a source at the ground, one uniformly
11 distributed through the canopy, and one decaying with depth in the canopy.
12 A fourth source type, where the in-canopy source depends on both the wind
13 speed and the difference in concentration between the canopy and a reference
14 concentration on the leaf, designed to mimic deposition, is also considered.

A. N. Ross

Institute for Climate and Atmospheric Science, School of Earth and Environment, Univ. of
Leeds, Leeds, UK.

I. N. Harman

CSIRO Oceans and Atmosphere Flagship, Canberra, Australia.

The simulations show that the topographically-induced perturbations to the scalar concentration and fluxes are quantitatively dependent on the source distribution. The net impact is a balance of different processes affecting both advection and turbulent mixing, and can be significant even for moderate topography. Sources that have significant input in the deep canopy or at the ground exhibit a larger magnitude advection and turbulent flux-divergence terms in the canopy. The flows have identical velocity fields and so the differences are entirely due to the different tracer concentration fields resulting from the different source distributions. These in-canopy differences lead to larger spatial variations in above-canopy scalar fluxes for sources near the ground compared to cases where the source is predominantly located near the canopy top. Sensitivity tests show that the most significant impacts are often seen near to or slightly downstream of the flow separation or reattachment points within the canopy flow. The qualitative similarities to previous studies using periodic hills suggest that important processes occurring over isolated and periodic hills are not fundamentally different. The work has important implications for the interpretation of flux measurements over forests, even in relatively gentle terrain and for neutral flow. To understand fully such measurements it is necessary not only to understand the flow structure (given the site characteristics) but also to know the distribution of scalar sources and sinks in the canopy.

Keywords Advection; Canopy; Complex terrain; FLUXNET; Scalar; Topography

1 Introduction

The issue of advection, or more strictly the divergence of the horizontal fluxes and transport by a mean vertical wind speed, has been an active area of research for some time (e.g., Aubinet et al, 2005; Feigenwinter et al, 2008; Zeri et al, 2010). Attempts to address the issue from an observational perspective have included the use of multiple towers (Feigenwinter et al, 2008), fully enclosed sampling methods (Leuning et al, 2008) and the development of algorithms to identify conditions when the eddy-covariance assumptions are not met (e.g., Goulden et al, 2006; van Gorsel et al, 2007, 2008), with mixed results. While much is known about the symptoms of advection, less is known about the underpinning physical or biophysical origins of the issue. In particular, while detailed analyses have been carried out at a number of sites, there remain key difficulties in taking the understanding gained and applying this to other sites. For example, Belcher et al (2012) note that the key diagnostic quantities and scales that determine the quantitative impact of the advection terms at any individual site are not really known. This is important as it would allow a more thorough analysis and quantification of the issue, e.g. determining defensible error estimates for the many hundred sites around the world and how this feeds through to the global and regional estimates of, for example, carbon exchange or ecosystem functioning. Such understanding could be used to develop site-diagnostic tools to assist in locating future FLUXNET sites.

A quantitative understanding of how the near-surface flow and turbulence responds to canopies and complex terrain is a necessary precursor to the un-

61 derstanding of how scalars are transported within that flow. This is in itself
62 challenging from an observational perspective (e.g., Zeri et al, 2010; Grant
63 et al, 2015). A range of methodologies have now been developed to quanti-
64 tatively describe the flow and turbulence, though most concentrate only on
65 neutral conditions. These include simple linearized theoretical approaches de-
66 veloped by Finnigan and Belcher (2004), Belcher et al (2008), Harman and
67 Finnigan (2013) and colleagues, and numerical simulations of varying degrees
68 of complexity (e.g., Ross and Vosper, 2005; Ross, 2008; Patton and Katul,
69 2009; Bohrer et al, 2009). Importantly, all of these studies indicate that the
70 presence of a canopy systematically alters the response of the flow to com-
71 plex terrain, both within and above the canopy, from the more traditional
72 understanding (Hunt et al, 1988; Belcher et al, 1993) even in gentle terrain.
73 These approaches show that the flow and turbulence vary systematically with
74 position in complex terrain, with hill crests particularly prone to significant
75 deviations in the flow vector and intensity of turbulence as compared to the
76 background state with no terrain.

77 A smaller number of studies have also considered the consequent impact on
78 the transport of scalars through that flow field from a more analytical perspec-
79 tive. Katul et al (2006) considered the transport of CO₂ emitted by a canopy,
80 with sources dictated by a full ecophysiological model as well as prescribed flux
81 and concentration boundary condition sources, in terrain comprised of simple,
82 repeating sinusoidal ridges. Ross (2011) considered the transport of a general
83 scalar emitted uniformly through a canopy again for sinusoidal ridges. More

84 recently Katul and Poggi (2010) considered the impact of complex terrain on
85 the deposition of aerosol-sized particles. The issue of inertial particle disper-
86 sion over complex terrain is also of increasing interest due to its importance
87 in the dispersion of seed kernels and vegetation migration, gene flow and pest
88 invasion (Katul and Poggi, 2012; Tracktenbrot et al, 2014). In all cases the
89 spatial variability in the flow and transport led to the systematic advection of
90 the scalar within and above the canopy and to spatial variability in the vertical
91 scalar flux that can be measured using the aerodynamic method. For the cases
92 considered the vertical scalar flux at twice canopy height varied by a factor
93 1.5–2 depending on position in both the Katul and Poggi (2010) and Ross
94 (2011) studies, certainly not insignificant. Katul and Poggi (2011) provided a
95 simple model to explain the aerosol deposition observed in Katul and Poggi
96 (2010). Ross (2011) attempted to place his results in a scaling framework (so
97 that the results can be generalized) although this is a partial analysis that
98 considers the impacts in the upper canopy only.

99 Scalars are, however, emitted or absorbed in a number of different ways
100 (passed through stomata, respired, deposited) leading to different source dis-
101 tributions and characteristics (prescribed fluxes, prescribed surface concen-
102 trations, mixed surface conditions) and a comparison of different scalars with
103 different source characteristics has not been undertaken to date. Raupach et al
104 (1992) showed that the perturbations to the scalar flux and concentration pat-
105 terns associated with flow over topography with low roughness are directly
106 controlled by the type of scalar source, so we should expect similar effects

107 when the topography is covered by a canopy. Furthermore the consideration
 108 solely of terrain with simple sinusoidal ridges ignores the fact that more re-
 109 alistic terrain could produce different impacts (usually smaller) with different
 110 spatial patterns (e.g., Harman and Finnigan, 2010). Here we seek to address
 111 two questions: firstly what role does source distribution play in governing the
 112 transport of scalars within and above canopies in complex terrain? Secondly,
 113 does the sinusoidal periodicity in the terrain considered to date affect our
 114 ability to draw general conclusions from more isolated hills?

115 **2 Methodology**

116 The conservation of a scalar tracer c in turbulent flow can be written as

$$\frac{\partial C}{\partial t} + U_j \frac{\partial C}{\partial x_j} = - \frac{\partial \overline{u'_j c'}}{\partial x_j} + S, \quad (1)$$

117 where c is the molar concentration, u_j is the wind vector and S is the source/sink
 118 of the scalar (zero above the canopy). Here the overline indicates both a tem-
 119 poral and local spatial average with upper case letters indicating the averaged
 120 quantity and primes the instantaneous and local deviations from the average.
 121 (A more rigorous discussion of the averaging procedure in canopies can be
 122 found in e.g. Finnigan, 2000). Molecular diffusion is neglected and the sum-
 123 mation convention assumed; S represents release/uptake of the scalar by the
 124 canopy. Equation 1 requires boundary conditions for solution, which permits
 125 further sources/sink terms at the boundaries e.g. to represent release/uptake of

126 the scalar by the soil. Alternatively concentration boundary conditions could
 127 be applied, although they are not considered further here.

128 In steady-state conditions, invoking continuity of the mean flow and ap-
 129 plying a first-order closure for the turbulent fluxes with isotropic diffusivity,
 130 K_c , Eq. 1 simplifies to

$$\frac{\partial C}{\partial t} = -\frac{\partial U_j C}{\partial x_j} + \frac{\partial}{\partial x_j} \left(K_c \frac{\partial C}{\partial x_j} \right) + S = 0. \quad (2)$$

131 Given forms for the mean wind field, U_j , the turbulent scalar diffusivity, K_c ,
 132 and the source/sink, S , Eq. 2 can be solved numerically to provide an estimate
 133 of the scalar concentration field.

134 The ratio of the turbulent momentum diffusivity, K_m to the turbulent
 135 scalar diffusivity defines the Schmidt number $S_c = K_m/K_c$. For neutral flow,
 136 observations suggest a value of ≈ 1 in the atmospheric boundary layer above
 137 the canopy, with values of ≈ 0.5 at canopy top (Raupach et al, 1996). Huang
 138 et al (2013) showed a connection between coherent canopy-flow structures and
 139 the turbulent Schmidt number in their large-eddy simulation study. Large-
 140 eddy simulations over flat ground by Ross (2008) showed reduced Schmidt
 141 numbers just above the canopy, but enhanced Schmidt numbers (up to about
 142 1.5) deeper within the canopy. The presence of a small hill led to variations
 143 in the Schmidt number across the hill, with larger values than occurred over
 144 flat ground at most locations and heights within and just above the canopy.
 145 With a mixing-length closure scheme the Schmidt number has to be specified.
 146 For simplicity, and in the absence of more detailed information on what the

147 correct Schmidt number should be in canopies over complex terrain, we take
148 $S_c = 1.0$ everywhere in this study.

149 Numerical solutions to this problem were found using the BLASIUS model
150 which has been used for a number of previous canopy-flow studies (e.g. Ross
151 and Vosper, 2005; Ross, 2011). The model solves the time dependent Boussi-
152 nesq equations in a terrain-following coordinate system and a 1.5-order tur-
153 bulence closure scheme is used. The flow is driven by an imposed pressure
154 gradient, balanced by a constant geostrophic wind (here taken as 10 m s^{-1}) at
155 the top of the model domain. The canopy is parametrized through a drag term,
156 $-c_d a \mathbf{u} |\mathbf{u}|$ in the momentum equation (where c_d is a local drag coefficient and
157 a is the leaf area density), a constant mixing length in the canopy and an en-
158 hanced dissipation rate due to the rapid conversion of energy from the large to
159 small scales by the work against canopy drag. Details of the scheme are given
160 in Ross and Vosper (2005). The canopy is parametrized in terms of the canopy
161 drag coefficient ($c_d = 0.25$), the canopy leaf area density ($a = 0.4 \text{ m}^{-1}$), the
162 canopy height $h_c = 10 \text{ m}$ and displacement height $d = 8.65 \text{ m}$. The canopy leaf
163 area density and canopy drag coefficient are assumed constant with height
164 in the canopy. While this is not completely realistic, Finnigan and Belcher
165 (2004) showed that this is a sufficient condition for first-order mixing-length
166 closure schemes to be a good approximation to a full second-order closure,
167 at least for the turbulent transport of momentum. Other relevant canopy pa-
168 rameters are derived using the relationship given in Ross and Vosper (2005),
169 so $l = \kappa(h_c - d) = 0.54 \text{ m}$ where κ is von Karman's constant, the canopy

170 adjustment length scale, $L_c = 1/(c_{da}) = 10$ m, and the momentum absorption
 171 efficiency $\beta \equiv u_\star/U_h = (l/(2L_c))^{1/3} = 0.3$, with u_\star the friction velocity and
 172 U_h the wind speed at canopy top when the canopy is on level ground. These
 173 canopy parameters are taken as fixed in all simulations presented here unless
 174 otherwise stated.

175 The model is run first as a one-dimensional (1-D) model to obtain a steady-
 176 state background profile (100000 s) and the results used to initialize a 2-D
 177 simulation, which is again run to steady state (1000 s). Initializing the 2-D
 178 simulation with the 1-D profile speeds up convergence in the 2-D simulation
 179 considerably. Periodic lateral boundary conditions are imposed, with a no-slip
 180 boundary condition at the floor of the canopy. The aerodynamic roughness
 181 length, $z_0 = 0.35$ m, is relatively high, but consistent with Ross and Vosper
 182 (2005). A domain depth of 1500 m is used, with a domain width of 2000 m
 183 while there are 80 grid points in the vertical with a stretched grid. The vertical
 184 resolution near the ground is 0.5 m with a stretch factor of 1.05, giving 12 grid
 185 points within the canopy for $h_c = 10$ m. At the upper boundary the geostrophic
 186 wind speed is prescribed.

187 In this study we consider the response of the scalar concentration field
 188 in idealized complex terrain, a single isolated two-dimensional ridge oriented
 189 normal to the geostrophic flow. The isolated ridge surface considered is given
 190 analytically by

$$z_{hill} = H \exp \{-x^2/L^2\}, \quad (3)$$

191 with $H = 10$ m and $L = 200$ m. This hill satisfies the small-slope conditions
192 of Finnigan and Belcher (2004) for their analytical model to be valid (the
193 maximum slope for these values of L and H is approximately 2.5°) though
194 not the restriction on canopy depth. The scaling arguments outlined in Ross
195 (2011) indicate that, for this hill-canopy combination, the scalar mean advec-
196 tion terms are small compared to the source strength. The horizontal domain
197 is 2000 m $= 10L$ and so the ridge can be considered isolated; there are 128
198 grid points in the horizontal and so the ridge is well resolved. In what follows
199 z is the vertical height above the surface and x is the horizontal position. The
200 velocity components u and w are the true horizontal and vertical velocities
201 respectively.

202 The primary focus here is the differing response of the scalar concentra-
203 tion profiles with position across complex terrain, as governed by different
204 source/sink profiles. All simulations are therefore performed with the same
205 canopy, hill and dynamical fields, but with various source / sink configurations.
206 In reality the sources and sinks of the important scalar species are driven by
207 a complex mix of physical and biological processes, including photosynthesis,
208 heterotrophic and autotrophic respiration and the surface energy balance. To
209 reduce this complexity we consider four stylized forms for the scalar source
210 distribution. Three of the sources are prescriptions of the flux and given ana-
211 lytically by

$$\begin{aligned}
S(x, z) &= \begin{cases} S_0/h_c & \text{if } z \leq h_c \text{ uniform source,} \\ S_0\alpha(z - h_c) \exp(z - h_c)/L_R & \text{if } z \leq h_c \text{ radiation source,} \end{cases} \\
\overline{w'c'}(z = 0) &= S_G \quad \text{ground source.}
\end{aligned} \tag{4}$$

212 These three forms for the source are canonical representations for condi-
213 tions when the scalar source is uniformly distributed through the canopy (as
214 in Ross, 2011), when the scalar source is controlled by a depth-varying process
215 similar to photosynthesis, and when the scalar source is located at the ground.
216 For ground sources the scalar roughness length associated with the boundary
217 layer is $z_{0c} = 0.05$ m. In Eq. 4 S_0 and S_G control the total source magnitude
218 (given in $\text{mol m}^{-2} \text{s}^{-1}$), L_R is a depth scale controlling the variation of the
219 source distribution within the canopy, and $\alpha(L_R)$ is a parameter used to scale
220 the source strength to ensure the depth-integrated source equals S_0 . These
221 three source profiles are particularly useful as their distribution bridges the
222 case where the source is predominately emitted in the upper canopy ('radia-
223 tion source' with L_R small) to the case where the scalar is entirely emitted
224 at the ground. The respective impacts on the scalar concentration with posi-
225 tion then provide insight into the relative importance of the different processes
226 involved in the flow transport of scalars in complex terrain.

227 The fourth scalar source considered is a prescription of the canopy-element
228 surface scalar concentration. The scalar source is then given by (Harman and

229 Finnigan, 2008)

$$S(x, z) = \frac{c_d a}{2} r |\mathbf{U}| (C(x, z) - C_0) \quad (5)$$

230 if $z \leq h_c$ (the rUC source), where C_0 is the element surface value of the
 231 scalar concentration and $r \approx 0.1$ is a leaf-level Stanton number. Unlike the
 232 prescribed sources in Eq. 4 the rUC source strength can vary with position
 233 (and even change sign) (see also Katul et al, 2006).

234 For all source types an equal and opposite sink term is distributed over a
 235 layer at the top of the domain in order to ensure the total scalar is conserved
 236 and hence a steady state is possible. There is zero scalar flux at the top of the
 237 domain.

238 In the next section we show how the scalar concentration varies with posi-
 239 tion across the specified isolated ridge and with source distribution.

240 **3 Results**

241 **3.1 Impact of scalar source distribution**

242 The importance of the source type and distribution is illustrated by simulat-
 243 ing the concentration fields and associated transport terms within the flow
 244 over a single isolated, gentle ridge covered by a uniform canopy with the dif-
 245 ferent sources described above. The canopy and flow parameters are fixed, as
 246 described above. For the three source terms with a prescribed flux we take
 247 $S_0 = S_G = 1 \text{ mol m}^2 \text{ s}^{-1}$ with $L_R = 1 \text{ m}$ for the radiation source. For the rUC
 248 source we take $r = 0.1$ and $C_0 = 100 \text{ mol m}^{-3}$. Figure 1 shows the background,

249 flat terrain, profiles of the source strength, the difference in scalar concentra-
250 tion from a reference value at height $z = 5h_c$, and the vertical turbulent scalar
251 flux as obtained with the mixing-length closure. The normalization scales are
252 the friction velocity u_* and turbulent scalar scale c_* as calculated from the
253 constant-flux layer just above the canopy. Despite the normalization, and that
254 three of the four cases have an identical depth-integrated source strength,
255 there is a difference in depth-integrated scalar concentration. This is because
256 the use of the first-order closure requires vertical gradients in the concentra-
257 tion sufficient to support the (prescribed) flux. Consequently, the cases where
258 the source is located in the upper canopy ('radiation' and 'rUC' cases) lead to
259 smaller gradients and differences in scalar concentration through the canopy.
260 For the case of the ground source, the turbulent diffusivity is so small near the
261 ground that significant gradients are required to support the flux. Given that
262 advection becomes a problem for eddy covariance in the presence of gradients
263 (in the wind field and/or concentration fields) then this suggests a priori that
264 estimates of the strength of ground-based sources are more likely to be affected
265 by advection than are upper canopy sources.

266 Figure 2 shows the results of the model for the streamwise component of
267 the wind vector (a), the vertical velocity (b) and the turbulent diffusivity K_c
268 (c) with position over the ridge. Note that, despite being of gentle slope, the
269 canopy height ($h_c = 10$ m) and canopy density scale ($L_c = 10$ m) are sufficient
270 to generate regions of reversed flow within the canopy, which are driven by the
271 balance between shear stress, aerodynamic drag and the hill-induced pressure

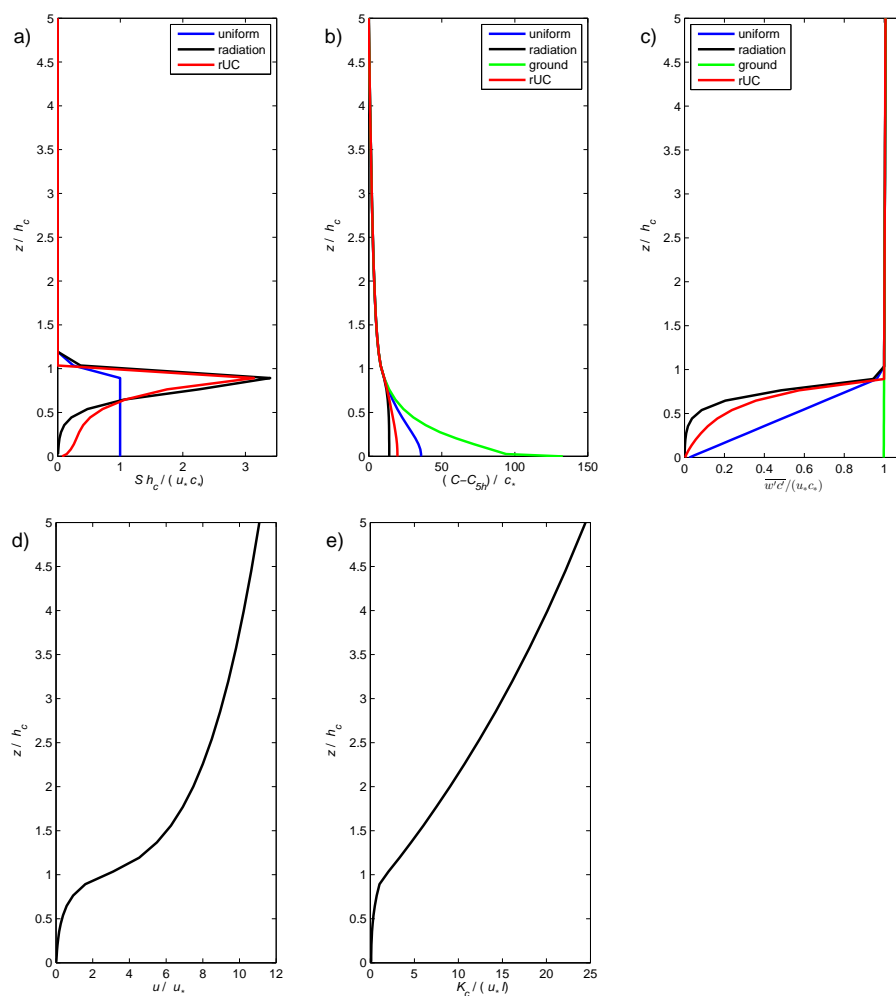


Fig. 1 Normalized background profiles of (a) scalar source term, (b) scalar concentration, (c) turbulent scalar flux in the absence of a hill, (d) horizontal velocity and (e) turbulent diffusivity. The lines in figures (a)-(c) are for the different sources: uniform (blue), radiation (black), ground (green) and rUC (red).

272 perturbation (Finnigan and Belcher, 2004), including well upstream from the
 273 ridge. The changes in the turbulent diffusivity across the ridge appear small,
 274 except in the deep canopy. However, as noted earlier, even small changes in

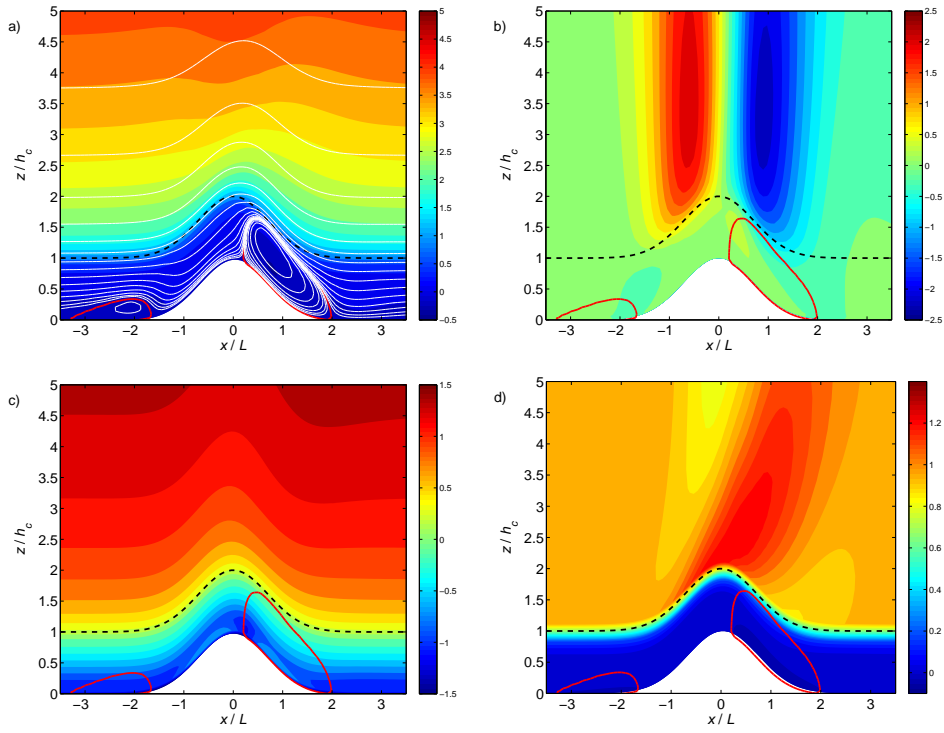


Fig. 2 Contour plots of the (a) normalized horizontal velocity, U/U_h , (b) normalized vertical velocity, $W/(U_h H/L)$, (c) normalized eddy viscosity, $K_c/(u_* l)$ on a \log_{10} scale and (d) the normalized vertical momentum flux, $\overline{u'w'}/(-u_*^2)$. The black dotted line marks the canopy top and the solid red line is the dividing streamline delineating regions of flow separation. The thin white lines on (a) show other streamlines of the flow, logarithmically spaced. Not all of the numerical domain is shown.

275 the diffusivity can lead to large changes in the scalar concentration profile and
 276 concentration gradients so these cannot be deemed inconsequential without
 277 further study. The diffusivity changes are mainly located near to the ground
 278 and originate from changes to the near-ground wind speed and the associated
 279 boundary layer.

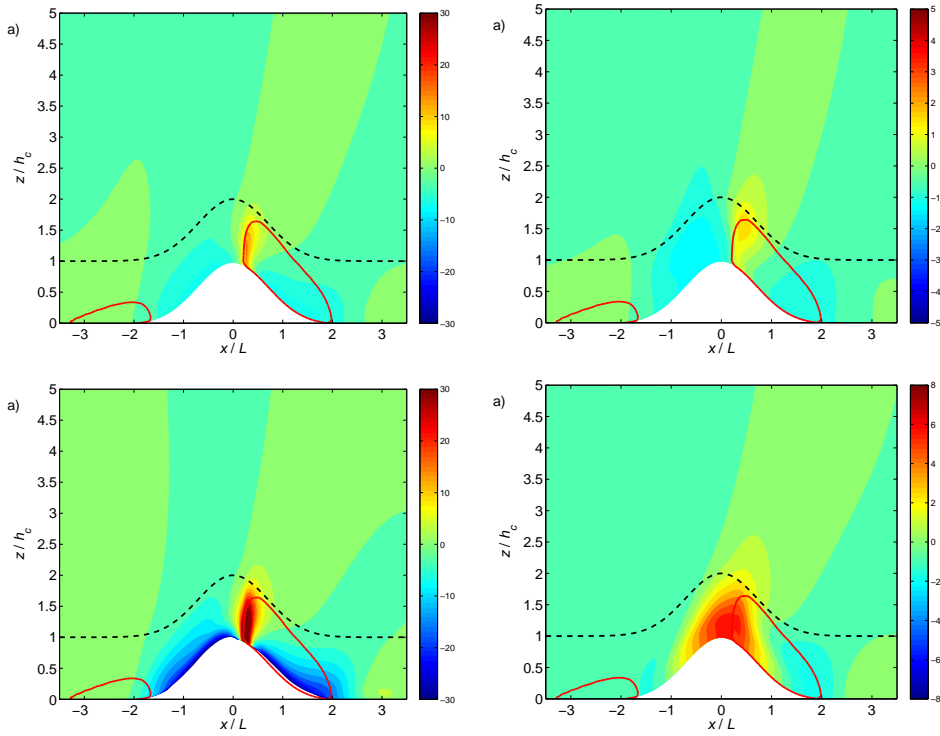


Fig. 3 Contour plots of scalar concentration perturbation fields (2-D minus 1-D field), normalized by c_* , for different source types: (a) uniform source, (b) radiation source, (c) ground source and (d) rUC source. The 1-D field is the steady state solution over flat terrain shown in Fig. 1. The black dotted line marks the canopy top and the solid red line is the dividing streamline delineating regions of flow separation. Note the different colour scales on the different subfigures.

280 Figures 3 and 4 show the steady-state fields of the normalized scalar con-
 281 centration difference and vertical scalar fluxes across the isolated ridge. Qual-
 282 itatively the pattern of the impact is similar across the four cases and also
 283 similar to the results shown in Katul et al (2006) and Ross (2011). In partic-
 284 ular the largest impacts are seen around the convergence/divergence zones in
 285 the simulated wind field (i.e. at hill crest and near the bottom of the ridge, see

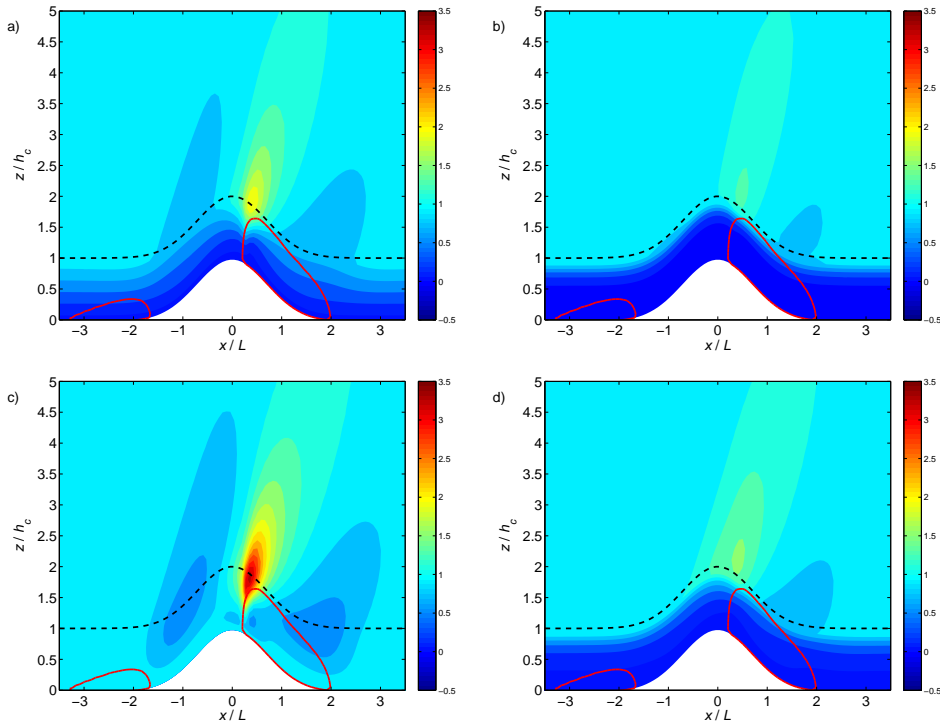


Fig. 4 Contour plots of vertical scalar turbulent flux normalized by $u_* c_*$, for different source types: (a) uniform source, (b) radiation source, (c) ground source and (d) rUC source. The black dotted line marks the canopy top and the solid red line is the dividing streamline delineating regions of flow separation.

286 Figs. 2 and 3). These are the regions with the largest vertical motion in the
 287 canopy that enables a systematic transport of air with different scalar concen-
 288 tration into/out of the canopy, and/or low values of the turbulent diffusivity
 289 within the canopy, which enables the establishment of large scalar concentra-
 290 tions for transport by the mean flow. From the streamlines it is clear that
 291 the vertical motion near canopy top is relatively weak for this hill, although
 292 it is more important deeper in the canopy in the proximity of the regions of

293 separated flow. Nonetheless it does have a marked effect in modulating scalar
294 concentrations across the hill.

295 Figure 5 shows the normalized vertical scalar flux at twice canopy height
296 (left) and three times canopy height (right) above the ground with position
297 across the hill for the four source distributions. This shows that, depending
298 on a) the tower location, and b) the source type and distribution, location-
299 specific observations of the vertical scalar flux can be significantly biased with
300 respect to the actual source strength. The spatial pattern is non-symmetric
301 around the value of 1 as a result of the background concentration profile and
302 the lack of vertical symmetry that leads to the regions of positive and neg-
303 ative vertical velocity being of different sizes. This asymmetry indicates that
304 local measurements of the vertical scalar flux somewhat underestimate the
305 true source strength as a consequence of the flow and transport except within
306 small regions where the observations provide a large overestimate. This im-
307 plies a general tendency to underestimate the scalar eddy-covariance flux from
308 towers randomly positioning in the landscape. Furthermore the local measure-
309 ments of scalars with ground-based sources are clearly more affected than
310 those with sources in the (upper) canopy. The different impacts on scalars
311 with different sources also suggest that knowledge about the likelihood of im-
312 pacts on one scalar cannot necessarily be used to infer impacts on other scalars
313 with different source/sink distributions (e.g. energy balance closure and CO₂
314 closure).

315 The scalar concentration and flux fields from different source distributions
316 can be superimposed if they are all prescribed by flux boundary conditions.
317 Figure 5 also shows horizontal profiles of the vertical turbulent flux across the
318 ridge for two cases with more realistic combined sources, i) ‘Balanced’ with
319 a ground source exactly balanced by a canopy sink (i.e. surface respiration
320 balancing net canopy assimilation) and hence the net source strength is zero;
321 ii) ‘Midday’ with a canopy sink strength that is three times that of a ground
322 source (i.e. typical of a midday balance of carbon sources/sinks) and hence the
323 net source strength is $-S_0$. For case (i) where there is no net source of scalar, a
324 non-zero local vertical flux is nevertheless observed across the ridge. Near the
325 region of flow separation this is significant (up to $0.9S_0$), with a smaller mag-
326 nitude negative flux balancing elsewhere over the slopes. This feature arises
327 because of the relatively larger impact on the scalar concentrations and flux
328 patterns for the ground source as compared to the radiation source. For case
329 (ii) with the same net source as before, the fact that the concentration associ-
330 ated with the ground source shows a much larger response to the ridge means
331 that it dominates the spatial patterns, even though it is smaller by a factor of
332 three than the radiation source term. The net effect depends on sensor height
333 and does not follow the pattern followed by either single source term. As the
334 balance between the different source changes, e.g. through the day or with
335 the season, the topographically-induced bias in local fluxes can therefore vary
336 significantly.

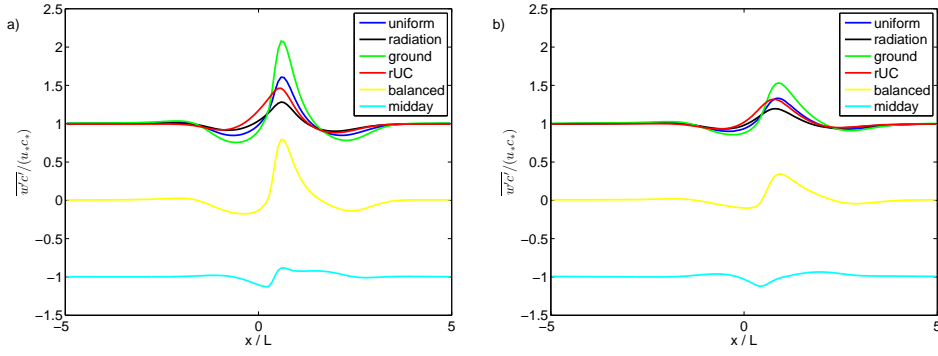


Fig. 5 Profiles of turbulent scalar flux normal to the mean flow at (a) height h_c and (b) height $2h_c$ above the canopy top for the different source types. In addition to the four standard source types, lines are also included for two combined sources. The first ('balanced') has equal and opposite ground source and radiation sink terms of strength S_0 , and therefore the net source term is zero. The second ('midday') mimics daytime photosynthesis and soil respiration and has a radiation sink of strength $-1.5S_0$, and a ground source term of strength $0.5S_0$. The net source is therefore equal to $-S_0$.

3.2 Budget analysis

To fully understand the origins of these results, especially with regard to their robustness to modelling specifics, it is useful to separate out the different terms in the scalar equation (Eq. 2) while Fig. 6 shows the horizontal and vertical components of the advection term ($\partial UC/\partial x$ and $\partial WC/\partial z$ respectively) as well as the total advection term ($\partial UC/\partial x + \partial WC/\partial z$) for the uniform source and the radiation source. Figure 7 shows the horizontal and vertical components of the turbulent flux divergence ($\partial \overline{u'c'}/\partial x$ and $\partial \overline{w'c'}/\partial z$). For large regions of the ridge and surroundings the divergence of both the turbulent flux and the mean advection terms are small. These small values however are necessary to

347 establish the spatial patterns in the scalar concentration and scalar turbulent
348 flux.

349 The individual advection terms in Fig. 6 are larger in magnitude, however
350 the horizontal and vertical components largely cancel out over most of the
351 flow-field (see e.g. Finnigan, 1999). If the advection terms are not written in
352 flux form (as in Eq. 1) then the individual terms are even larger (not shown).
353 The net effect of advection is therefore a balance of two large, but largely
354 cancelling, terms. To observe the advection terms in the field it is therefore
355 necessary to carefully measure both horizontal and vertical advection terms
356 and to do so to a high level of accuracy to ensure the net sum is accurately
357 calculated.

358 In contrast, around the regions of convergence in the U field, both advec-
359 tion and turbulent flux divergence are large. In the region of the separation
360 point near the hill crest these patterns arise from the streamwise convergence
361 of the mean flow and scalar enriched air within the canopy ($\partial UC/\partial x < 0$),
362 with corresponding transport by the mean flow vertically (and a mean flux
363 divergence $\partial WC/\partial z > 0$). Following the mean flow, the scalar enriched air
364 is transported upwards into the upper canopy where it is rapidly mixed due
365 to increased turbulence. Consequently, the vertical turbulent flux is increased
366 markedly and associated gradients in all four transport terms occur (and in
367 particular $\partial WC/\partial z < 0$ and $\partial \overline{w'c'}/\partial z > 0$). Similar, but countersigned, argu-
368 ments lead to the patterns at the base of the ridge in Figs. 6 and 7, with the
369 reduced magnitude due to the natural vertical asymmetry in the background

370 scalar concentration and proximity to the ground. Qualitatively the results in
371 Fig. 6 are similar to those presented in Katul et al (2006) despite the analytical
372 flow field, but more complicated ecophysical source model, used in that study.

373 While both the uniform and radiation sources lead to broadly similar pat-
374 terns in the advection and turbulent flux divergence, there are some important
375 quantitative differences between the two cases, despite both having identical
376 velocity fields. The most noticeable feature is that the magnitudes of the ad-
377 vection and turbulent flux-divergence terms are smaller with the radiation
378 source. There are also differences in the location of the maximum in the advec-
379 tion terms. The differences are due to the different scalar concentration fields
380 resulting from the different source distributions. With the radiation source
381 located in the upper canopy the scalar concentrations and vertical scalar gra-
382 dients are smaller in the deep canopy than in the constant source case, and
383 so advection plays a lesser role here. Instead, with the radiation source, the
384 advection term is most important in the upper canopy where the largest scalar
385 gradients occur. The individual, and largely cancelling, horizontal and vertical
386 components of the advection terms look quite similar between the two cases,
387 but the sum of the terms shows distinctive patterns near canopy top, again
388 highlighting the difficulties in measuring the effect of advection in the field.
389 A similar pattern to the net advection is seen in the vertical turbulent flux
390 divergence term.

391 Turbulent transport is dominated by the vertical term. The horizontal
392 turbulent flux-divergence term is largest near the leading edge of the separation

393 bubble, and even there it is two orders of magnitude smaller than the vertical
394 turbulent-flux divergence. This is in line with scaling arguments and previous
395 work (Finnigan, 1999) and suggests that from an observational point of view
396 it is not necessary to measure these terms, at least for a passive scalar.

397 Both the advection and perturbations to the turbulent divergence terms
398 are only (really) large in the convergence/divergence zones within the canopy.
399 This implies that these could be, a) sensitive to the numerical schemes used, b)
400 sensitive to resolution, and c) sensitive to the turbulence parametrization. We
401 expect flow separation to be a ubiquitous feature of canopy flows over hills. The
402 analytical model of Finnigan and Belcher (2004) shows this to be driven by the
403 adverse pressure gradient over the lee slope that is, to leading order, an inviscid
404 process and therefore insensitive to the details of the turbulence scheme. The
405 qualitative physical reasoning is therefore robust and so we would expect to
406 see a similar balance of terms to that shown here, although the precise details
407 may be dependent on the model specifics.

408 3.3 Sensitivity to model parameters

409 There are a number of non-dimensional parameters (h_c/L_c , L_c/L , H/L , h_c/H)
410 controlling the flow and scalar transport over idealized forested ridges such
411 as these. The sensitivity of the results to the three independent parameters
412 (L_c/L , h_c/L_c and H/L) is investigated through a series of simulations. The
413 canopy density remains fixed throughout so L_c is unchanged. To vary L_c/L
414 both L and H are changed keeping h_c/L_c and H/L fixed and to vary h_c/L_c

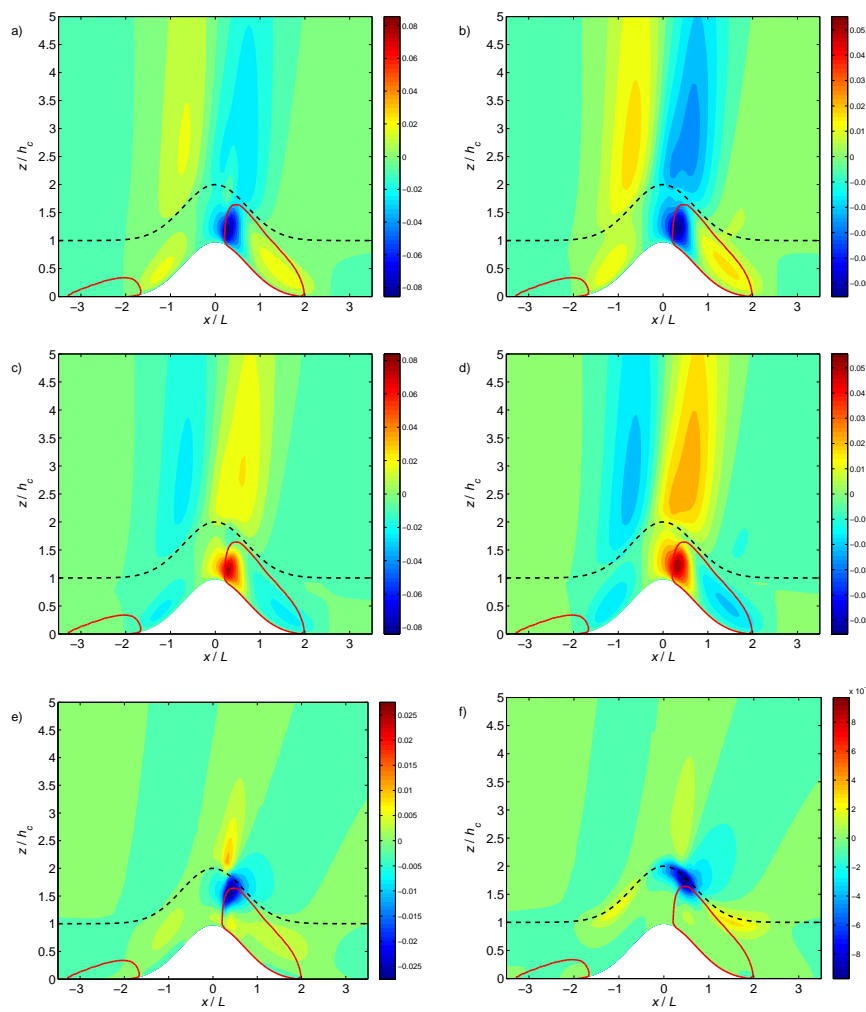


Fig. 6 Contour plots of horizontal scalar advection (a,b), vertical scalar advection (c,d) and total scalar advection (e,f) terms for the uniform source (a,c,e) and the radiation source (b,d,f). The black dotted line marks the canopy top and the solid red line is the dividing streamline delineating regions of flow separation. Note the different colour scales in each plot.

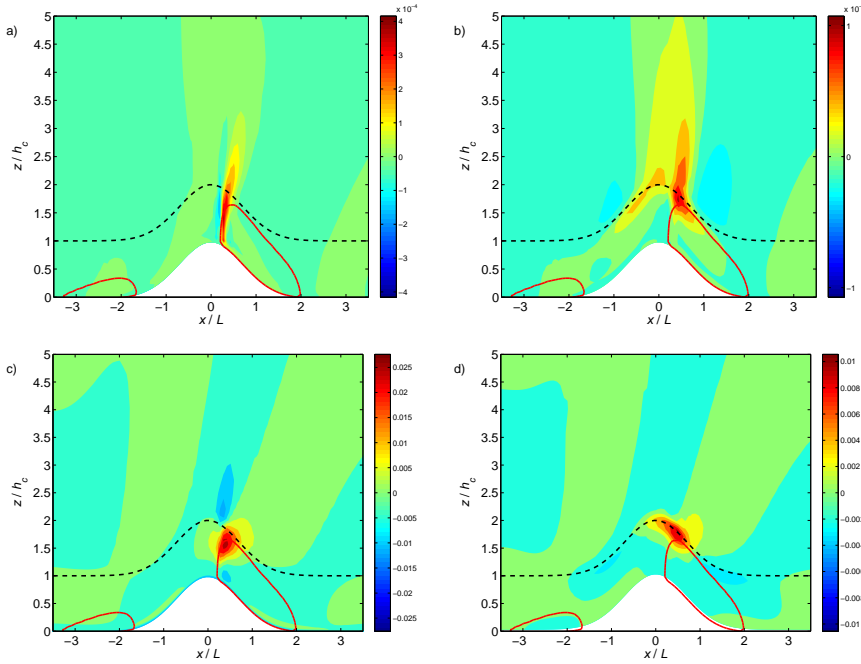


Fig. 7 Contour plots of perturbations in the horizontal (a,b) and vertical (c,d) turbulent scalar flux divergence terms for the uniform source (a,c) and the radiation source (b,d). The black dotted line marks the canopy top and the solid red line is the dividing streamline delineating regions of flow separation. Note the different colour scales in each plot.

415 the canopy height h_c is changed with the hill remaining fixed. Changes in H/L
 416 are made by changing H . In all these simulations the unchanged parameters
 417 take the same values as given in Sect. 2. For simulations where L was varied,
 418 the width of the domain and the number of horizontal gridpoints were scaled
 419 with L to ensure that the horizontal resolution remained constant. In each
 420 case the magnitude and location of the maximum and minimum of the scalar
 421 flux term at height h_c above the canopy is plotted as a function of the varying
 422 non-dimensional parameter (L/L_c , h_c/L_c and H/L) (see Fig. 8).

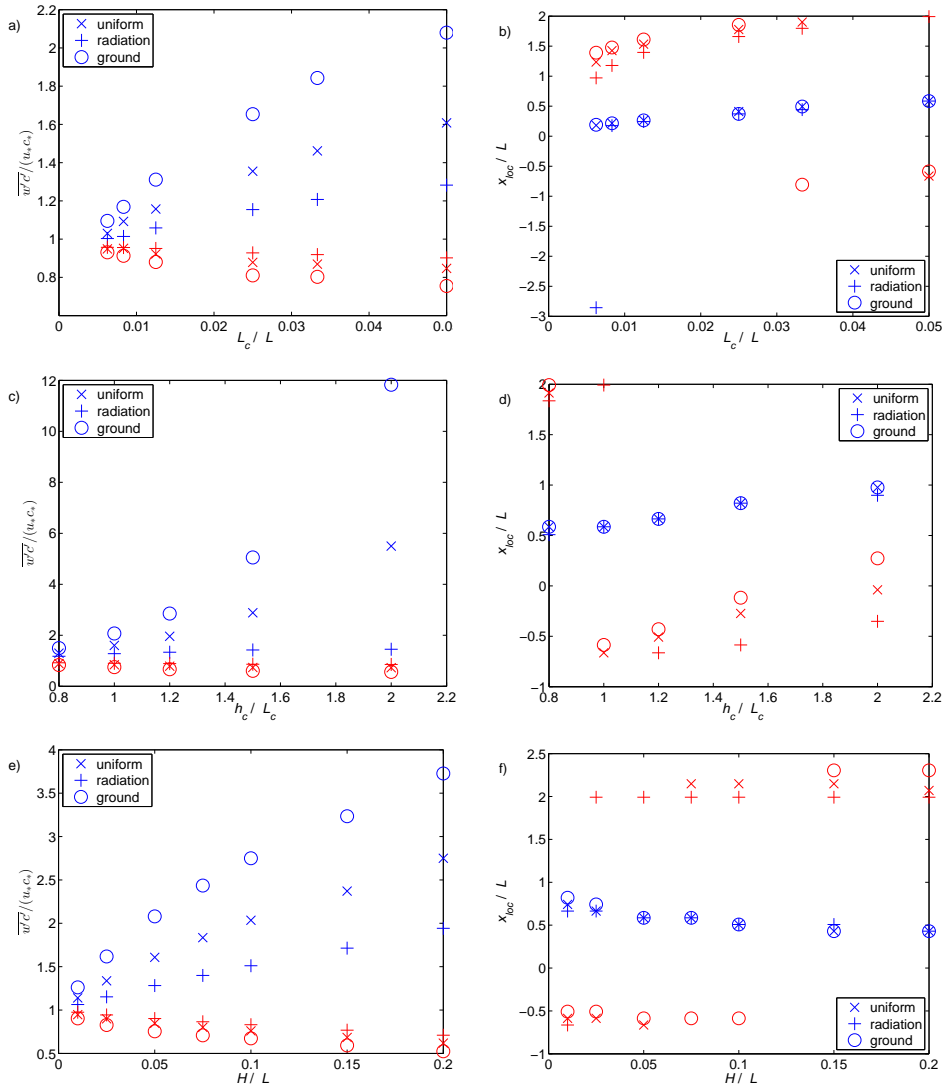


Fig. 8 Plots of the magnitude (a, c, e) and location, x_{loc} , (b, d, f) of the maximum (blue) and minimum (red) turbulent scalar flux normal to the mean flow at a height of h_c above the canopy as a function of L_c/L (a, b), h_c/L_c (c, d) and H/L (e, f). The different source distributions are marked with different symbols.

423 The maximum and minimum changes in the above-canopy scalar flux in-
424 crease with increasing L_c/L , h_c/L_c and H/L . In each case increasing the
425 non-dimensional parameter leads to an increase in the induced flow pertur-
426 bation, and hence an increase in the scalar-flux perturbations. The dynamical
427 changes are, at least qualitatively, entirely consistent with the dependence of
428 the perturbed flow on L_c/L , h_c/L_c and H/L seen in the analytical solution
429 of Finnigan and Belcher (2004) and in the numerical simulations of Ross and
430 Vosper (2005) over infinite periodic hills. Variations in the location of the
431 flow separation and reattachment points, which are key to understanding the
432 changes to the scalar fluxes, are due to second-order terms as discussed in Ross
433 and Vosper (2005) and Harman and Finnigan (2013). The pattern of ground
434 sources having more impact than radiation sources on the above-canopy flux
435 perturbations for a given canopy and hill is a consistent feature across all
436 these simulations. The location of the maximum canopy flux is strongly tied
437 to regions of the flow where $\partial U/\partial x < 0$, for example the flow separation point
438 just downwind of the hill summit. In these sensitivity tests the only case for
439 which the maximum is not located at the flow separation point is for the ra-
440 diation source and the smallest value of L_c/L . In this case the perturbed flow
441 and the changes in the scalar flux are negligible anyway. The flux minimum
442 is often located near the re-attachment point of the flow over the lee slope.
443 There is also a local above-canopy flux minimum over the upwind slope where
444 penetration of the mean flow into the canopy reduces the scalar concentration
445 gradient and the turbulent flux above the canopy. Both of these are associated

446 with $\partial U/\partial x > 0$. For some non-dimensional parameter values the minimum on
447 the upwind slope can be the global minimum in the above-canopy scalar flux.
448 Which of the two local minima is more significant appears to vary smoothly
449 with the non-dimensional parameters. Small L_c/L , small h_c/L_c and large H/L
450 tend to lead to the minimum near the re-attachment point being most signif-
451 icant, while the upwind minimum dominates for large L_c/L , large h_c/L and
452 small H/L values. The precise transition point between these two behaviours
453 depends not just on the dynamics, but also on the source distribution, with
454 the ground sources tending to undergo transition earlier to an upwind flux
455 minimum becoming dominant.

456 Overall this sensitivity analysis shows that, as might be expected, the mag-
457 nitude of the effects increases as the flow perturbations induced by the hill
458 increase (narrow hills, deeper canopies, steeper slopes). The flow separation
459 point is almost always important, particularly for controlling where the max-
460 imum observed fluxes are located. Minimum values can be due to either flow
461 into the canopy near the re-attachment point, or alternatively due to the mean
462 flow into the canopy over the upwind slope, particularly when the induced flow
463 is larger. In these idealized simulations these appear to be robust features of
464 the flow over a range of canopy and hill parameters and also different source
465 terms. Of course, in reality we know that flow separation and re-attachment
466 is unsteady and sensitive to other processes such as stratification and canopy
467 density in the trunk space (see e.g., Belcher et al, 2008; Patton and Katul,
468 2009; Poggi and Katul, 2007) and so these results cannot be directly used

469 to assess if a particular time period of scalar-flux measurement is affected by
470 these processes. The present results do however provide a qualitative indica-
471 tion of the likely effects of complex terrain on above-canopy scalar fluxes over
472 a range of conditions.

473 **4 Discussion**

474 From the results presented here it is clear that the location of sources or
475 sinks in a forest canopy over complex terrain has a significant impact on the
476 above canopy variability in scalar concentrations and fluxes. Sources that are
477 at the surface (ground source), or inject a significant amount of the scalar in
478 to the deep canopy (uniform source), lead to greater variability compared to
479 those sources where the scalar is predominantly injected in the upper canopy
480 (radiation and rUC sources).

481 To understand this we first consider the case over flat ground where the
482 steady-state scalar profile can be understood as a simple balance between the
483 source term and the scalar turbulent flux divergence in the canopy (advection
484 plays no role in a steady 1-D solution). Sources with significant input of scalar
485 in to the deep canopy require there to be a flux divergence in the deep canopy
486 (assuming a flux-gradient relationship holds). This requires a large vertical
487 gradient in the scalar concentration field since the turbulent diffusivity is low
488 in the deep canopy.

489 For the 2-D case, the steady-state scalar solution is a subtle balance be-
490 tween the source, the turbulent scalar-flux divergence and the scalar advection

491 terms. The presence of a hill induces non-linear flow perturbations in the deep
492 canopy that are large compared to the background flow, and so variations
493 in the eddy diffusivity and advection are much more important for sources
494 near the ground. Hence these sources display the largest variations in scalar
495 concentration and turbulent fluxes.

496 The variations in scalar concentration and wind speed across the hill can
497 have some impact on the total source from the canopy with sources that depend
498 on the atmospheric scalar concentration. For example, with the ‘rUC’ source
499 there is a 2.3% increase in the average scalar source compared to that from
500 a canopy over flat ground. This is small, but not negligible, and is due both
501 to changes in U and C . Locally, changes in the source term are larger, as
502 shown in Fig. 9. In absolute terms the ‘rUC’ source is largest near the top of
503 the canopy and decays with depth as U decreases. In relative terms, however,
504 the biggest effect is seen deeper in the canopy over the ridge slopes. Over both
505 the upwind and lee slopes there is a marked increase in the source term by
506 up to a factor of three due to the induced flow in the canopy over the hill. In
507 contrast, there is a decrease in the source in the upper canopy over the lee slope,
508 again driven primarily by the reduction in wind speed in the upper canopy
509 (see Fig. 2a). Obviously this is a simple idealization of the actual response of
510 photosynthesis to changes in CO_2 concentration in a canopy but, consistent
511 with Katul et al (2006), it suggests that the dynamics of canopy flow over
512 complex topography can have a direct influence on the total CO_2 uptake by

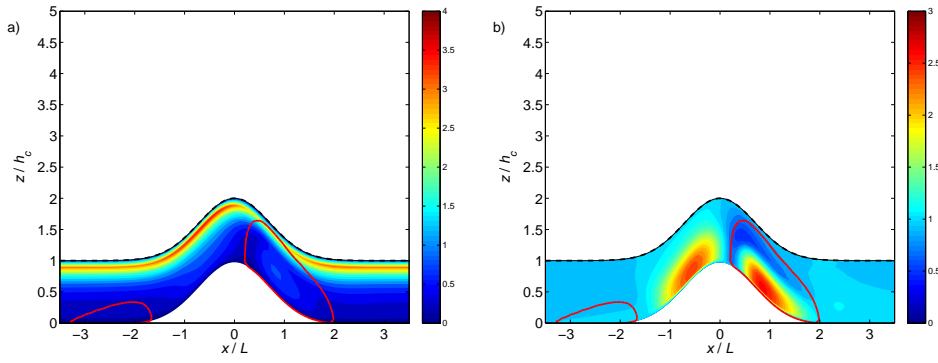


Fig. 9 Contour plots of (a) tracer source term, $S(x, z)$, for the rUC source and (b) normalized source term, $S(x, z)/S_{1d}(z)$, for the rUC source, where $S_{1d}(z)$ is the source term for a flat, homogeneous canopy.

513 the forest, aside from any physiological changes due to other ambient changes
 514 in climate (e.g. temperature or wind speed with height).

515 The differences in fluxes persist to several canopy heights, and so there
 516 are important implications of these results for interpreting flux measurements
 517 from single towers and scaling them to estimate total forest sources and sinks
 518 of CO_2 and other scalars (as noted by Ross, 2011). Estimating net ecosystem
 519 exchange (NEE) at flux-tower sites also requires an estimate of the changes
 520 in CO_2 storage within the canopy, often achieved using a profile of high reso-
 521 lution concentration measurements. The advection terms may also affect such
 522 estimates of NEE through two additional processes. In steady flow, changes
 523 in the storage at a particular location may not be representative of the whole
 524 canopy because of the inhomogeneity of the scalar field. Furthermore, changes
 525 in storage may often be accompanied by changes in the mean flow and turbu-
 526 lence, which will probably result in changes to the scalar concentration pat-

527 terns and scalar advection. Such changes will depend on the site, the canopy
528 and on the meteorological conditions and so will likely need to be considered
529 on a case-by-case basis. All this is for neutral flow and for very small hills,
530 and is therefore separate to the well-documented issues related to drainage
531 flows and nocturnal flux measurements. Ross (2011) gave a scaling analysis
532 to estimate the impact of this effect for a uniform scalar source and for given
533 canopy parameters. Here we show that knowing the details of the canopy is
534 not sufficient. Different source distributions produce different responses above
535 the canopy (see Fig. 5), even for the same total source strength, and so in
536 order to interpret flux measurements from above the canopy one must know
537 something about the source distribution in addition to the canopy structure.
538 This is a challenging requirement.

539 In contrast to previous studies (e.g., Ross, 2011), our study uses an iso-
540 lated ridge rather than periodic terrain. While this makes some quantitative
541 difference to the results, the qualitative picture is unchanged, with the largest
542 perturbations to the scalar concentration being observed near the stagnation
543 point, just downstream of the summit, and the largest scalar fluxes being ob-
544 served above the upper part of the lee slope. Further down the lee slope, and
545 over the upwind slope, fluxes above the canopy are actually slightly reduced.
546 The effect of the hill on the fluxes can be observed up to $3L$ upwind of the
547 summit and $3.5L$ downwind of the summit at a height of $2h_c$. At a height
548 of $3h_c$, the impact on the fluxes is smaller, but the effects are seen even fur-
549 ther downwind, up to $4L$ from the summit. At a distance of $4L$ the ridge has

550 reduced to 1/16 of its peak height. To avoid the effects of the ridge on flux
551 measurements instruments should be located away from the summit.

552 One potential limitation of this work is the assumption that we can use
553 a simple mixing-length turbulence closure for the turbulent transport of mo-
554 mentum and scalars within the canopy. There are acknowledged failings of
555 mixing-length closures in strongly distorted flows, or in canopies with rapid
556 changes in foliage distribution (see e.g Finnigan et al, 2015, for discussion).
557 Finnigan and Belcher (2004) showed theoretically that, for turbulent transport
558 of momentum, the closure assumptions are reasonable for a uniform canopy
559 density. Momentum fluxes are most significant in the upper canopy where the
560 closure assumptions hold well. There is more uncertainty in the lower canopy,
561 however typically velocities and velocity gradients are small there and so mo-
562 mentum transport is not significant anyway. The situation is slightly more
563 complicated for scalar transport, since there may be significant scalar concen-
564 tration gradients lower down in the canopy, particularly for ground sources.
565 This introduces a quantitative uncertainty into these results, however the key
566 physical processes controlling the variations in scalar concentration and fluxes,
567 namely flow deceleration and flow separation, are essentially inviscid processes
568 driven by the hill-induced pressure gradient (Finnigan and Belcher, 2004). One
569 would therefore expect to see qualitatively similar results with different tur-
570 bulence closure schemes.

571 We finally reiterate that these simulations consider topography that would
572 not usually be considered complex by the eddy-covariance community and are

573 for neutrally stratified flow. These results are primarily the consequence of the
574 additional physical processes that occur when the canopy flow interacts with
575 topography. Isolated two-dimensional topography results in a larger magnitude
576 of the hydrodynamic pressure perturbation than for isolated three-dimensional
577 topography for the same hill characteristics (e.g., Hunt et al, 1988). Boundary-
578 layer flow is inevitably somewhat unsteady in wind direction and speed that
579 tends to smooth out topographically-locked flow features (e.g., Patton and
580 Katul, 2009). Hence it is to be expected that these simulations overstate the
581 topographic impacts on the transport of scalars at real sites. Nevertheless,
582 the magnitude of the simulated impact is not trivial nor would these impacts
583 necessarily be obvious without additional observational constraints.

584 There are then clear pressing knowledge gaps for the eddy-covariance com-
585 munity that are raised by this study. The first is an ability to routinely assess
586 whether a particular site is potentially affected by advection and to place er-
587 ror bounds on the possible impacts. Scale analysis (Ross, 2011) while helpful
588 will not necessarily identify suitable sites, given the fine balance of physical
589 processes occurring (there are at least five independent length scales to the
590 problem). This is separate from, but related to, requirements around instru-
591 mentation footprints in complex terrain (e.g., Finnigan, 2004). Second, and
592 far more challenging, is an ability to correct existing data for the impacts of
593 topographic/complex terrain effects. The assimilation of eddy-covariance data
594 into a simple flow-transport model provides one potential method for achieving
595 this aim.

596 **5 Conclusions**

597 Returning to our initial questions we conclude that, 1) source distribution plays
598 a critical role in determining the modelled patterns of scalar concentrations
599 and fluxes over hills covered by tall canopies, and 2) the scalar fields modelled
600 here over an isolated ridge are qualitatively similar to those seen in previous
601 studies with periodic ridges. The scalar fields are dominated by flow-related
602 changes in the turbulent mixing and the flow separation within the canopy over
603 the lee slope. Earlier conclusions around scalar transport in complex terrain
604 (e.g. around scaling arguments) are thus more widely applicable to a range of
605 hill geometries.

606 The topographic impacts on scalar concentrations and vertical fluxes are
607 strongly dependent on the distribution and type of sources contributing to the
608 scalar. The relative impact is larger for scalars with sources near the ground
609 since the topography has a relatively larger impact on the flow and turbulence
610 field near the ground. The net topographic impact on scalars with multiple
611 sources (e.g. net canopy CO₂ assimilation and ground respiration) is sensitive
612 to the balance in distribution and strength of the sources, so assessing possible
613 errors using simple rules-of-thumb is not practical. For scalars whose sources
614 are determined through concentration boundary conditions (and by inference
615 mixed boundary conditions, e.g., temperature or water vapour), correlations
616 in space between the flow perturbations and the scalar concentrations lead
617 to spatial variations in the source strength that can be sufficient to lead to

618 a landscape-averaged source strength that differs from the background, no-
619 terrain, case.

620 The topographic impacts simulated are seen even for very gentle topogra-
621 phy (slopes of $\approx 2.5^\circ$ are considered) and can occur well away from topography
622 (discernible impacts occur up to $2.5L$ away from ridge crest) and in neutrally
623 stratified flow. The inherent smoothing that occurs with long-time averaging,
624 including over wind direction, will tend to reduce the potential for biases in
625 eddy-covariance estimates of scalar exchange over complex terrain but cannot
626 guarantee to remove all such biases. We have considered purely the impacts
627 of topography on short-time period concentrations and fluxes. The variability
628 and sensitivity in the impacts will be manifest as variability in the longer-
629 term relationships between scalar exchanges and their climatological drivers.
630 We conclude that eddy-covariance data require interpretation within the to-
631 pographic context at all sites.

632 **Acknowledgements** We would like to thank John Finnigan and Eva van Gorsel for useful
633 discussions.

634 **References**

635 Aubinet M, Berbigier P, Bernhofer CH, Cescatti A, Feigenwinter C, Granier A,
636 Grünwald TH, Havrankova K, Heinesch B, Longdoz B, Marcolla B, Montag-
637 nani M, Sedlak P (2005) Comparing CO₂ storage and advection conditions
638 at night at different CARBOEUROFLUX sites. *Boundary-Layer Meteorol*
639 116:63–94, DOI 10.1007/s10546-004-8

- 640 Belcher SE, Newley TMJ, Hunt JCR (1993) The drag on an undulating surface
641 induced by the flow of a turbulent boundary layer. *J Fluid Mech* 249:557–
642 596, DOI 10.1017/S0022112093001296
- 643 Belcher SE, Finnigan JJ, Harman IN (2008) Flows through forest canopies in
644 complex terrain. *Ecol Apps* 18:1436–1453, DOI 10.1890/06-1894.1
- 645 Belcher SE, Harman IN, Finnigan JJ (2012) The wind in the willows: Flows
646 in forest canopies in complex terrain. *Annu Rev Fluid Mech* 44:479–504,
647 DOI 10.1146/annurev-fluid-120710-101036
- 648 Bohrer G, Katul GG, Walko RL, Avissar R (2009) Exploring the effects of
649 microscale structural heterogeneity of forest canopies using large-eddy sim-
650 ulations. *Boundary-Layer Meteorol* 132(3):351–382, DOI 10.1007/s10546-
651 009-9404-4
- 652 Feigenwinter C, Bernhofer C, Eichelmann U, Heinesch B, Hertel M, Janous
653 D, Kolle O, Lagergren F, Lindroth A, Minerbi S, Moderow U, Mölder
654 M, Montagnani L, Queck R, Rebmann C, Vestin P, Yernaux M, Zeri M,
655 Ziegler W, Aubinet M (2008) Comparison of horizontal and vertical ad-
656 vective CO₂ fluxes at three forest sites. *Agric For Meteorol* 148(1):12–24,
657 DOI 10.1016/j.agrformet.2007.08.013
- 658 Finnigan JJ (1999) A comment on the paper by Lee (1998) "On micromete-
659 orological observations of surface-air exchange over tall vegetation". *Agric*
660 *For Meteorol* 97:55–64, DOI 10.1016/S0168-1923(99)00049-0
- 661 Finnigan JJ (2000) Turbulence in plant canopies. *Annu Rev Fluid Mech*
662 32:519–571, DOI 10.1146/annurev.fluid.32.1.519

- 663 Finnigan JJ (2004) The footprint concept in complex terrain. *Agric For Me-*
664 *teorol* 127:117–129, DOI 10.1016/j.agrformet.2004.07.008
- 665 Finnigan JJ, Belcher SE (2004) Flow over a hill covered with a plant canopy.
666 *Q J R Meteorol Soc* 130:1–29, DOI 10.1256/qj.02.177
- 667 Finnigan JJ, Harman IN, Ross AN, Belcher SE (2015) First order turbulence
668 closure for modelling complex canopy flows. *Q J R Meteorol Soc* submitted
- 669 van Gorsel E, Leuning R, Cleugh HA, Keith H, Suni T (2007) Nocturnal
670 carbon efflux: Reconciliation of eddy covariance and chamber measure-
671 ments using an alternative to the u^* -threshold filtering technique. *Tellus*
672 *B* 59(3):397–403, DOI 10.1111/j.1600-0889.2007.00252.x
- 673 van Gorsel E, Leuning R, Cleugh HA, Keith H, Kirschbaum MUF, Suni T
674 (2008) Application of an alternative method to derive reliable estimates
675 of nighttime respiration from eddy covariance measurements in moder-
676 ately complex topography. *Agric For Meteorol* 148(6-7):1174–1180, DOI
677 10.1016/j.agrformet.2008.01.015
- 678 Goulden ML, Miller SD, da Rocha HR (2006) Nocturnal cold air drainage and
679 pooling in a tropical forest. *J Geophys Res - Atmospheres* 111(D8):D08S04,
680 DOI 10.1029/2005JD006037
- 681 Grant ER, Ross AN, Gardiner BA, Mobbs SD (2015) Field observations of
682 canopy flow over complex terrain. *Boundary-Layer Meteorol Online* First:1–
683 21, DOI 10.1007/s10546-015-0015-y
- 684 Harman IN, Finnigan JJ (2008) Scalar concentration profiles in the canopy
685 and roughness sublayer. *Boundary-Layer Meteorol* 129(3):323–351, DOI

686 10.1007/s10546-008-9328-4

687 Harman IN, Finnigan JJ (2010) Flow over hills covered by a plant canopy:

688 Extension to generalised two-dimensional topography. *Boundary-Layer Me-*

689 *teorol* 135(1):51–65, DOI 10.1007/s10546-009-9458-3

690 Harman IN, Finnigan JJ (2013) Flow over a narrow ridge covered with a plant

691 canopy: A comparison between wind-tunnel observations and linear theory.

692 *Boundary-Layer Meteorol* 147(1):1–20, DOI 10.1007/s10546-012-9779-5

693 Huang J, Katul G, Albertson J (2013) The role of coherent turbulent structures

694 in explaining scalar dissimilarity within the canopy sublayer. *Env Fluid*

695 *Mech* 13:571–599, DOI 10.1007/s10652-013-9280-9

696 Hunt JCR, Leibovich S, Richards KJ (1988) Turbulent shear flow over low

697 hills. *Q J R Meteorol Soc* 114:1435–1470, DOI 10.1002/qj.49711448405

698 Katul GG, Poggi D (2010) The influence of hilly terrain on aerosol-sized par-

699 ticle deposition into forested canopies. *Boundary-Layer Meteorol* 135:67–88,

700 DOI 10.1007/s10546-009-9459-2

701 Katul GG, Poggi D (2011) A note on aerosol sized particle deposition onto

702 dense and tall canopies situated on gentle cosine hills. *Tellus B* 63:395–400,

703 DOI 10.1111/j.1600-0899.2011.00528.x

704 Katul GG, Poggi D (2012) The effects of gentle topographic variation on

705 dispersal kernels of inertial particles. *Geophys Res Lett* 39:L03401, DOI

706 10.1029/2011GL050811

707 Katul GG, Finnigan JJ, Poggi D, Leuning R, Belcher SE (2006) The influence

708 of hilly terrain on canopy-atmosphere carbon dioxide exchange. *Boundary-*

-
- 709 Layer Meteorol 118:189–216, DOI 10.1007/s10546-005-6436-2
- 710 Leuning R, Zegelin SJ, Jones K, Keith H, Hughes D (2008) Measurement of
711 horizontal and vertical advection of CO₂ within a forest canopy. *Agric For*
712 *Meteorol* 148:1777–1797, DOI 10.1016/j.agrformet.2008.06.006
- 713 Patton EG, Katul GG (2009) Turbulent pressure and velocity perturbations
714 induced by gentle hills covered with sparse and dense canopies. *Boundary-*
715 *Layer Meteorol* 133:189–217, DOI 10.1007/s10546-009-9427-x
- 716 Poggi D, Katul GG (2007) Turbulent flows on forested hilly terrain: the recir-
717 culation region. *Q J R Meteorol Soc* 133:1027–1039, DOI 10.1002/qj.73
- 718 Raupach MR, Weng WS, Carruthers DJ, Hunt JCR (1992) Temperature and
719 humidity field and fluxes over low hills. *Q J R Meteorol Soc* 118:191–225,
720 DOI 10.1002/qj.49711850403
- 721 Raupach MR, Finnigan JJ, Brunet Y (1996) Coherent eddies and turbulence
722 in vegetation canopies: the mixing length analogy. *Boundary-Layer Meteorol*
723 78:351–382, DOI 10.1007/978-94-017-0944-6_15
- 724 Ross AN (2008) Large eddy simulations of flow over forested ridges. *Boundary-*
725 *Layer Meteorol* 128:59–76, DOI 10.1007/s10546-008-9278-x
- 726 Ross AN (2011) Scalar transport over forested hills. *Boundary-Layer Meteorol*
727 141:179–199, DOI 10.1007/s10546-011-9628-y
- 728 Ross AN, Vosper SB (2005) Neutral turbulent flow over forested hills. *Q J R*
729 *Meteorol Soc* 131:1841–1862, DOI 10.1256/qj.04.129
- 730 Tracktenbrot A, Katul GG, Nathan R (2014) Mechanistic modeling of seed
731 dispersal by wind over hilly terrain. *Ecol Modelling* 274:29–40, DOI

732 10.1016/j.ecolmodel.2013.11.029

733 Zeri M, Rebmann C, Feigenwinter C, Sedlak P (2010) Analysis of short periods

734 with strong and coherent CO₂ advection over a forested hill. *Agric For*

735 *Meteorol* 150(5):674–683, DOI 10.1016/j.agrformet.2009.12.003